Applied Thermal Engineering 210 (2022) 118403

Contents lists available at ScienceDirect

Applied Thermal Engineering

journal homepage: www.elsevier.com/locate/apthermeng

Research Paper

Defining the cooling and heating solar efficiency of a building component skin: application to a modular living wall

Z. Azkorra-Larrinaga *, A. Erkoreka-González, I. Flores-Abascal, E. Pérez-Iribarren, N. Romero-Antón

ENEDI Research Group, Department of Energy Engineering, University of the Basque Country UPV/EHU, Alda. Urquijo s/n, 48013 Bilbao, Spain

ARTICLE INFO

Keywords:
Cooling efficiency
Energy performance
Energy saving
Modular Living Wall

ABSTRACT

The thermal evaluation of building components composed of a base wall with a solar passive skin solution, such as a vertical/roof greenery system, ventilated façade, reflective painting, etc., is usually performed as a whole. In this research, it has been proven that, independently of the base wall thermal inertia and insulation level, the temperature of the outermost surface layer of any building component during sunny hours is mainly dependent on the ambient air temperature and relative humidity, the incident global solar radiation and the building skin behaviour.

The latter assumption has been proven on the south wall of a reference building simulated with TRNSYS. The south wall properties have been varied and the building has been subjected to different climates. The assumption's validity has been checked for twelve south wall cases: a combination of 2 thermal transmittance, 2 thermal inertia and 3 climates. Each case has been simulated for a whole year. Based on this finding and the local ambient conditions for sunny hours, the hypothetical achievable maximum and minimum temperatures for the outermost surface layer have been defined. Then, based on the outermost surface temperature experimental measurements, the cooling and heating solar efficiencies valid for any skin solution have been defined.

Furthermore, the developed methodology has been applied to a vertical living wall tested for a whole year under the accuracy and quality procedure of the PASLINK method. In this way, the cooling and heating solar efficiencies were experimentally determined for this skin solution for both, the hot cold seasons. The study has shown that the cooling efficiency during the hot season is 90.8%. As expected, even during sunny summer hours, the presence of water positively affects the performance of the façade, as it brings the base wall external surface temperature close to the ambient wet bulb temperature, therefore reducing the cooling load of the building. For the cold season, the cooling efficiency was similar, at 90.3%, which means a heating efficiency of 9.7%. Again, even for sunny winter hours, the values of the external surface temperature tend towards the ambient air wet bulb temperature, resulting in an increase in the heating demand.

These experimental efficiency values allow the heating or cooling behaviour of different skin solutions to be comparable with a single number that is independent of the base wall composition. In addition, independently of the base wall composition, once the experimental efficiency value of a given skin solution is known, it allows (during sunny hours) the base wall outermost surface temperature to be calculated with precision. The latter makes it possible to increase the accuracy of the estimation of the heating and cooling demands of such methods as the degree-day method.

1. Introduction

Nowadays, population growth and urbanization in cities is affecting the quality of life in the European Union (EU). Buildings make up 40% of energy consumption and generate 36% of CO_2 emissions in the EU, according to 'H2020 Energy Efficient Buildings (EeB)" [1]. The building sector is a key element to help decarbonise Europe, reducing its CO_2 emissions by 80% and energy consumption by 50% by 2050. Most buildings in Europe (both residential and tertiary) were built without considering their energy efficiency a priority [2].

Therefore, energy efficiency in buildings is part of a global 2030 strategy concerning energy use in a society which is betting strongly on sustainable development as a way to ensure a future where the living

* Corresponding author.
E-mail address: zaloa.azkorra@ehu.eus (Z. Azkorra-Larrinaga).

https://doi.org/10.1016/j.applthermaleng.2022.118403
Received 13 August 2021; Received in revised form 12 February 2022; Accepted 21 March 2022
Available online 24 March 2022

Nomenclature

C	Volumetric heat capacity (MJ/(m^{3}K))
e	Thickness of homogeneous layer (m)
G	Global solar radiation on a vertical plane (W/m^2)
h	Convective heat transfer coefficient (W/(m^2 K))
k	Thermal conductivity coefficient (W/(m K))
i	Number of sublayers
q	Heat flux (W/m^2)
RH	Relative humidity (%)
T	Temperature (°C)
U	Thermal transmittance (W/(m^2 K))

Greek symbols

α	Absorptivity (–)
ε	Emissivity (–)
σ	Stefan-Boltzmann constant ($5.67 \bullet 10^{-8}$ W/(m^2 K^4))

Abbreviations

BW	Bare wall
CRES	Centre for Renewable Energy Sources and Saving
EU	European Union
GF	Green Façade
GR	Green Roofs
LCCE	Laboratory for Quality Control in Buildings of the Basque Government
LW	Living Wall
MLW	Modular Living Wall
UTC	Coordinated Universal Time
VGS	Vertical Greenery Systems

Subscripts

abs	Absorbed
atm	Atmospheric
base, summer	Base temperature for summer
base, winter	Base temperature for winter
comb	Combined
cond	Conduction
conv	Convective
evap	Evaporation
max	Maximum value
min	Minimum value
in	Indoor
lw	Long-wave radiation
out	Outdoor
rad	Radiation
sat	Saturation
sol–air	Solar -air (temperature)
surf	Surface (homogeneous layer outer surface)
surr	Surrounding surfaces
sw	Short-wave radiation

conditions of the population should always be within comfort levels, without an irreversible negative influence on the environment caused by human activity [3].

While the installation of other heating or cooling system options are costly and time consuming, passive technologies for urban green infrastructures, such as green roofs (GR) and vertical greenery systems (VGS), can improve the thermal performance of building envelopes more economically [4].

One type of VGS is a modular living wall (MLW), where plants are grown on vertical surfaces, with the substrate standing vertically in modules, is a relatively new application of VGS using modern technology [5]. Common systems for living walls are modular, panel or felt systems. Modular systems are pre-planted modules that are attached to the structures. A watering and nutrient distribution system is always required and the modular panels should be replaceable [6].

While VGS have been in use for centuries, there has recently been a surge in interest in installing them in both retrofit and new construction applications. The potential benefits of VGS include their aesthetic appeal [7], improved indoor air quality [8], improved outdoor air quality [9], habitats for animals [10], sound attenuation [11,12], reduction of the "heat-island effect" in cities [13–15], storm water reduction [16] and energy savings.

The thermal performance of VGS and its impact on building's heating and cooling demands has been extensively quantified in both experiments and mathematical modelling. Perini et al. [17] shows a temperature reduction at the VGS in a range of 2–6 °C compared with the bare wall (BW). Eumorfopoulou and Kontoleon [18] also measured temperature differences in a green façade (GF) and found that the minimum and maximum surface temperatures of a GF are considerably lower than those of the BW sections. In a similar study Yin et al. [19] results show that the daily surface temperature in a GF is significantly lower than the average BW surface temperature, with a maximum reduction of 4.67 °C, and that the cooling effect of the GF is most obvious in the middle of the day and significantly decreases at night. Another recent study by Shafiee et al. [20] found that a living wall (LW) can reduce the ambient air temperatures by up to 8.7 °C, reducing the temperature fluctuations by decreasing the maximum and increasing the minimum temperatures of the ambient air close to the façade.

In addition to work on the effects of the ambient temperature reduction that can be obtained from VGS, some research has been carried out on the insulation benefits that green walls can provide.He and Jim [21] evaluates the thermodynamic transmission in a GR using a simulation model based on the traditional Bowen ratio energy balance model (BREBM). It determined that the GR absorbs and stores large amounts of heat to form an effective thermal insulation against fluctuations. Further research by Pérez et al. [22] show VGS as passive energy-saving systems thanks to the shade produced by the vegetation and the insulation provided by the vegetation and substrate. Another recent work of research, Fox et al. [23], found that diurnal fluctuations in the heat flux were lower for the LW system than without it. Nayak et al. [24] focused on a full-scale comparison of a double-skin GF with a LW. The results showed a high energy saving potential during the cooling season for the LW (58.9%) compared to (33.8%) for the double-skin green façade.

With respect to predictive models of the energy performance of VGS, several studies have used field measurements to parameterize simplified mathematical models [25]. Each of these studies have made simplifications with respect to the effects of evapotranspiration and time-varying soil thermal properties. The evaporation ratio can be defined as a function of the water content of the surface layer [26]. Both studies were also limited in scope to the air conditioning energy saving potential in summer.

A physics based model of the energy balance of a GR has been developed and integrated into the EnergyPlus building energy simulation programme [27]. Sailor found that building energy consumption varies significantly in response to variations in growing media depth, irrigation and vegetation density.

Apart from Sailor, some other researchers have simulated GR and have validated Sailor's model with experimental data [28,29], obtaining relatively accurate values of the soil's outer surface temperature for such a complex model.

The Sailor model is based on the [30,31] models on GR and

highlights all the heat and mass transfer processes that happen in the GR. As noted above, these processes are coupled to each other, as it is hard to investigate them separately. Some researchers, such as Feng et al. [32], developed a model of the photosynthesis and transpiration processes, calculating their effect on the energy balance of the GR. Kumar and Kaushik [33] studied the air temperature inside the foliage and modelled it. Ayata el at. [34] carried out some experiments to decouple the sensitive heat transfer process in the GR and evaluate it separately. Some investigations [35,36] have been carried out to examine the soil layer's thermal conductivity and thermal capacity variation with the soil moisture content. Chiba et al. [37] conducted an experimental study on the effect that a VGS has on the heat transfer coefficient of buildings. It concluded that the vertical greenery system (VGS) allows energy consumption to be minimized during summertime.

The energy performance in buildings is influenced by many factors, and this complex situation makes it very difficult to accurately implement the prediction of building energy consumption [38]. So it is also important to note that there are some other approaches to the GR thermal behaviour by other authors, such as the modelling approach in [21] that treat the GR as a radiation shield. The modelling approach in [39] also uses differential equations, but the assumptions are different compared to the Sailor model. There are also a couple of authors who have tried to simplify the GR model: [40,41], showing that relatively simple models can give accurate results [42]. Finally, Kotsiris et al. [43] tests a GR in the Greek PASLINK test site of The Centre for Renewable Energy Sources and Saving (CRES) and characterizes the GR with a factor named 'dynamic U-value' by the authors which depends on the behaviour of the GR; that is, it assumes that the improvement of the GR can be introduced as a reduction of the overall U-value of the whole roof.

The first aim of the study herein presented focuses on defining the solar cooling or heating efficiency valid for any skin solution of a building component. The method assumes (by proving its weight is negligible during sunny hours) that it is possible to neglect the term of heat transfer by conduction in the energy balances of the outermost surface of the façade, and thus estimate this surface temperature without considering it. Based on this assumption, it is possible to define a solar cooling and heating efficiency for any skin solution installed in the outermost layer of a building envelope and design a simple experimental test to obtain it. Thus, for sunny hours, the thermal behaviour improvement of including complex skin solutions as VGS, ventilated façades, or reflective painting solutions over traditional base wall finishing solutions could be comparable with a unique experimental value. The second aim of this study is to test the repeatability of the proposed efficiency value by experimentally obtaining the solar cooling and heating efficiency of a MLW innovative skin solution tested in a PASLINK test cell for a whole year.

2. Material and method

2.1. Defining the heating and cooling solar efficiency of the skin solution of a building component

A common method used to estimate the heating and cooling demands of a building is the degree-days methodology with ASHRAE Standard 90.1 [44]. For a common building component such as the one represented in Fig. 1, the heat flux associated with the steady-state heating demand due to transmission heat losses for a specific hour of a winter period would be calculated using equation (1):

$$\dot{q} = U\cdot\left(T_{base,winter} - T_{out}\right) = \frac{T_{base,winter} - T_{out}}{\frac{1}{h_{in}} + \sum_{i=1}^{n}\frac{e_i}{k_i} + \frac{1}{h_{out}}} = \frac{T_{base,winter} - T_{out}}{R_{in-out}} \quad \left[W/m^2\right] \tag{1}$$

where T_{out} is the outdoor temperature [°C], $T_{base,winter}$ is the base temperature for winter [°C], e_i is the thickness of the i^{th} layer of the building component [m], k_i is the thermal conductivity of the i^{th} layer [W/(m K)], and h_{in} and h_{out} are the internal and external surface convection-radiation combined heat transfer coefficients, respectively [W/(m^2 K)]. The indoor and outdoor convection-radiation heat transfer coefficients are usually fixed by the regulations, for example, in the Spanish Building Technical Code (CTE) [45] this value is fixed for vertical building components at h_{in} = 7.69 W/(m^2 K) and h_{out} = 25 W/(m^2 K).

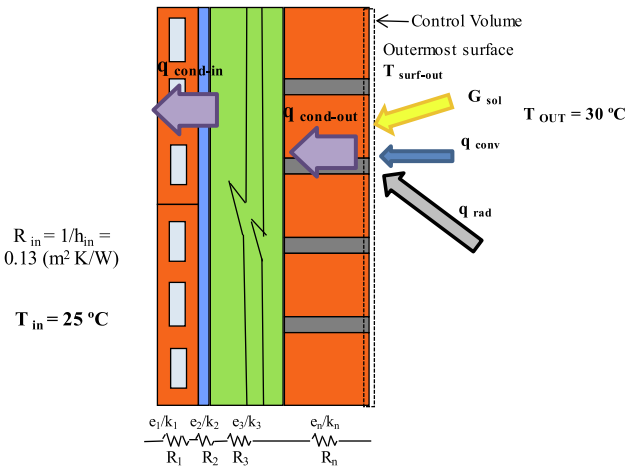

Fig. 1. Representation of a general n layer building component for a summer period.

For a specific hour of a summer period, the cooling demand associated with the steady-state transmission heat gains would be calculated using equation (2):

$$\dot{q} = U\cdot\left(T_{out} - T_{base,summer}\right) = \frac{T_{out} - T_{base,summer}}{\frac{1}{h_{in}} + \sum_{i=1}^{n}\frac{e_i}{k_i} + \frac{1}{h_{out}}} = \frac{T_{out} - T_{base,summer}}{R_{in-out}} \quad \left[W/m^2\right] \tag{2}$$

where $T_{base,summer}$ is the base temperature for summer [°C].

If we analyse Fig. 1 together with equation (1) and equation (2), it can be seen that the heat transfer phenomena occurring from the outermost surface of the building component towards the exterior, are the ones introducing the highest uncertainties in the degree-day methodology. In other words, the short-wave radiation exchange is considered in a very simple manner by assuming the effects of the solar gains within the base temperature. Solar gains effect within the building heating and cooling demands could be better estimated if the solar radiation effect on the building component's external surface temperature could be estimated accurately. That is, the outermost surface of a building component might be several degrees Celsius higher, during sunny hours, than the outdoors air temperature, yet equations (1) and (2) always use the outdoor air temperature for the heat transfer calculation.

Thus, if the outermost surface temperature of the building component were known during the sunny hours of the whole year, the equations (1) and (2) could use $T_{surf,out}$ in the calculations instead of T_{out}. Then the solar gains effect would be accurately calculated by equations (1) and (2), while the heating and cooling demands associated to transmissions losses/gains through the opaque part of the building envelope would also be precisely estimated.

A general n layer common building component can be seen in Fig. 1. If the external surface temperature of the building component were known, the steady-state equation of heat flux from this outermost surface towards the interior would be very easily calculated by equation (3):

$$\dot{q} = \frac{T_{surf-out} - T_{in}}{\sum_{i=1}^{n}\frac{e_i}{k_i} + \frac{1}{h_i}} = \frac{T_{surf-out} - T_{in}}{R_{in-surf,out}} \quad \left[W/m^2\right] \tag{3}$$

where $T_{surf\text{-}out}$ is the outermost surface temperature [°C], T_{in} is the indoor air temperature [°C], e_i is the thickness of the i^{th} layer of the building component [m], k_i is the thermal conductivity of the i^{th} layer [W/(m K)], and h_i is the internal surface convection-radiation combined heat transfer coefficient [W/(m^2 K)].

Before developing the methodology for $T_{surf,out}$ estimation through an experimentally obtained parameter, the layer where $T_{surf,out}$ will be estimated must be clearly defined. The position of $T_{surf,out}$ is clear in a common building component such as the one presented in Fig. 1, where the outermost layer is a facing brick or other skin finishing where only short-wave radiation heat transfer, long-wave radiation heat transfer and convective heat transfer occur with the exterior. In this case, the $T_{surf,out}$ position is the outermost surface where the heat transfer phenomena towards the interior of the building is converted into pure conduction through opaque layers. For these opaque layers, the thermal resistance should be estimated as e_i/k_i (see equation (3)). Unventilated air chambers, or other layers that can be modelled accurately with an equivalent thermal resistance, are equivalent to layers that can be represented in equation (3) as e_i/k_i.

In building components equipped with skins such as living walls or ventilated façades, where complex heat transfer phenomena, such as evapotranspiration and natural and/or forced ventilation, can occur in the outermost air chamber, the selection of the layer where $T_{surf,out}$ should be estimated must follow the same logic. This outermost surface layer must be the one from which only heat transfer by conduction will occur until the heat reaches the interior of the building. Then, if the $T_{surf,out}$ were known, the heat flux through the building component with this complex behaving skin could be accurately modelled by equation (3). As an example, a schematic of a building component with a green cover installed over a facing brick with a 5 cm ventilated air chamber is shown in Fig. 2. In this building component, with a modular living wall finishing skin, the $T_{surf,out}$ would be defined as the temperature of the outermost surface of the facing brick. Even in such a complex building component, if $T_{surf,out}$ were known for all the sunny hours of the cooling season, the cooling effect of the green cover could be accurately estimated by means of the simple equation (3). Although very complex heat transfer phenomena occur in the building envelope skin, from the layer defined as $T_{surf,out}$ in Fig. 2 towards the interior, through the layers 1 to 4, pure heat conduction can be assumed for the heat flux estimation and equation (3) could be accurately used.

Thus, if this outermost surface temperature during the sunny hours of the day could be estimated by a single performance parameter, then methods such as the degree-day method could be modified to estimate the cooling demand reduction potential of building component skins such as VGS during sunny hours. A similar approach could be done for building skin solutions with the aim of reducing the heating demand by trying to maximize this outermost surface layer temperature during sunny hours. Furthermore, this performance indicator should be valid for comparing the behaviour of different building component skin solutions for both, façades and roofs.

Here, the concept of building component skin solar efficiency can be defined as in equations (4) and (5), depending on whether it is characterized for the cooling season (4) or the heating season (5). See also Fig. 3 for clarification of equations (4) and (5).

The cooling or heating efficiency value is applicable to both walls and roofs subject to the incident solar radiation. These efficiency values relate the real experimentally measured $T_{surf\text{-}out}$ during sunny hours in the outermost surface of a building component with the maximum or minimum achievable temperatures in the outermost surface façade/roof of the building envelope, depending on the locally measured weather conditions:

$$\varepsilon_{cooling} = \frac{T_{max} - T_{surf-out}}{T_{max} - T_{min}} \quad [-] \tag{4}$$

$$\varepsilon_{heating} = \frac{T_{surf-out} - T_{min}}{T_{max} - T_{min}} \quad [-] \tag{5}$$

where:

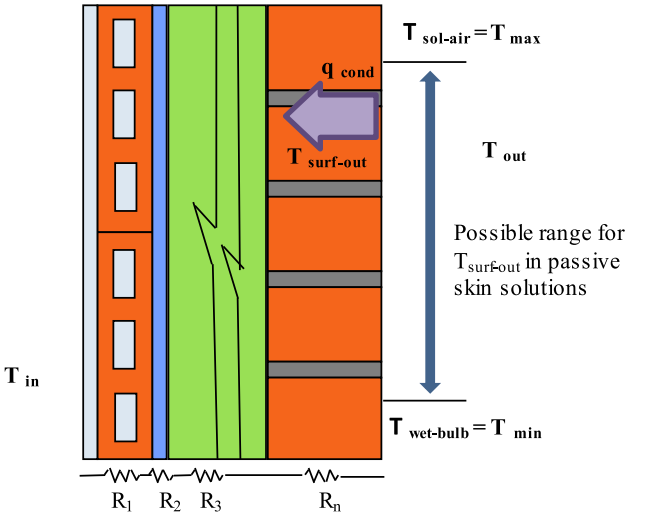

Fig. 3. Representation of T_{max}, T_{min} and $T_{surf-out}$ in a general n layer building component.

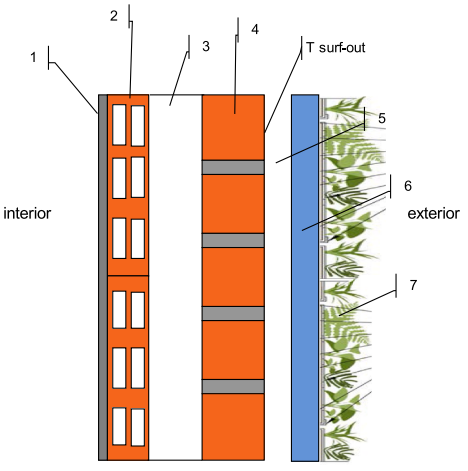

1. Cement mortar 1.5 cm
2. Hollow double brick 6.4 cm
3. Non-ventilated air chamber 10 cm
4. Facing brick 10.5 cm
5. Ventilated air chamber 5 cm
6. Pre-cultivated modules with substrate and irrigation system
7. Plants- evergreen shrub

Fig. 2. Detail of the composition of the tested MLW.

- T_{max} and T_{min} are the hypothetical limiting maximum and minimum achievable outermost surface temperatures, estimated using locally measured weather variables and specific algorithms.
- The maximum achievable temperature of the outermost surface of a building component facing solar radiation (T_{max}) will be estimated using the upper limit values of the ASHRAE sol–air temperature ($T_{sol-air}$) method [44].

$$T_{max} = T_{sol-air} = T_{out} + \frac{\alpha \cdot G_{sol}}{h_{comb}} - \frac{\varepsilon \cdot \Delta R}{h_{comb}} \quad [^{\circ}C] \tag{6}$$

where, α is the absorptivity of the surface for solar radiation; G_{sol} is the global solar radiation incident on the surface [W/m^2]; h_{comb} is the combined coefficient of heat transfer by long-wave radiation and convection at the outer surface [W/(m^2 K)]; T_{out} is the outdoor air temperature [°C]; ε is the hemispherical emissivity of the surface (-), and ΔR is the difference between long-wave radiation incident on the surface from the sky and the surroundings and the radiation emitted by a hypothetical blackbody at outdoor air temperature [W/m^2].

According to ASHRAE [44], the maximum possible $T_{sol-air}$ temperature is obtained when:

- The term $\frac{\alpha}{h_{comb}}$ has a value of 0.052, which represents the usual maximum value for this term.
- The term $\frac{\varepsilon \cdot \Delta R}{h_{comb}}$ has a value for horizontal surfaces facing the sky of 4 °C and for vertical surfaces of 0 °C.

- T_{min} is considered to be the wet bulb temperature, calculated using the locally measured outdoor temperature and humidity. T_{min}, is defined as the temperature of the air when it is adiabatically saturated with water, in which case its temperature will decrease to the temperature called wet bulb temperature [46]. The wet bulb temperature is always lower than the dry bulb temperature, except for those cases where the relative humidity is 100%, when they are equal. The wet bulb temperature can be calculated as a function of the outdoor air temperature and the relative humidity, using the following empirical algorithm [47].

$$T_{min} = T_{wet-bulb} = T_{out}\ atan\left[0.151977\ (RH\% + 8.313659)^{\frac{1}{2}}\right] + atan\ (T_{out} + RH\%) - \tan\ (RH\% - 1.676331) + 0.00391838\ (RH\%)^{\frac{3}{2}} atan\ (0.023101 RH\%) - 4.686035 \quad [^{\circ}C] \tag{7}$$

- $T_{surf-out}$ is the measured temperature of the outermost surface of a tested building component with a certain skin solution. It could be a façade or a roof component. To obtain the skin solution cooling solar efficiency using equation (4), the building component with the skin solution to be evaluated should be tested during several days facing south, if it is a façade solution, or facing the sky if it is a roof component.

It can be easily demonstrated by combining the previous cooling efficiency (equation (4)) and heating efficiency (equation (5)) the following relation between both efficiencies (equation (8)):

$$\varepsilon_{heating} = 1 - \varepsilon_{cooling} \quad [-] \tag{8}$$

The temperatures in the outermost surface T_{max} and T_{min} represent the worst and best scenarios of the building component skin behaviour depending on the season considered. In summer, the worst condition happens when the surface temperature ($T_{surf-out}$) is the maximum possible (T_{max}), and the best condition happens when $T_{surf-out}$ reaches T_{min}. On the contrary, in winter, the façade should work in the opposite way.

The proposed method relies on the validity of the following strong assumption: "during sunny hours of the day where the global solar radiation striking on the outermost surface of a building component is over 150 W/m^2, the conduction heat transfer mechanism occurring through the $T_{surf,out}$ layer can be considered negligible in comparison with the sum of the short-wave solar radiation, long-wave radiation and convective heat exchanges occurring in the building skin".

If this strong assumption is valid, once a building skin efficiency is obtained by means of a testing campaign, where the building skin has been installed in a specific building component with a $\sum_{i=1}^{n} \frac{e_i}{k_i}$ value and the test has been carried out with a specific T_{in}, the efficiency values obtained for the building skin solution by means of equations (4) and (5) would be valid to estimate the $T_{surf,out}$ values of this skin solution when installed in any other building component, even working with a different T_{in} value. The $T_{surf,out}$ values for a skin solution for which the cooling solar efficiency ($\varepsilon_{cooling}$) has been obtained through an experimental campaign, when installed in another building component with a $\sum_{i=1}^{n} \frac{e_i}{k_i}$ value different from the one used during the testing campaign, would be estimated as in equation (9):

$$T_{surf-out} = T_{max} - \varepsilon_{cooling} \cdot (T_{max} - T_{min}) \quad [^{\circ}C] \tag{9}$$

where $\varepsilon_{cooling}$ is the one obtained during the testing campaign, T_{max} would be obtained by applying equation (6) with the local weather conditions of the new location where the building skin is to be installed, and T_{min} would be obtained by applying equation (7) with the local weather conditions of the new location where the building skin is to be installed.

The selection of the lower limit of 150 W/m^2 for the incident global solar radiation for the efficiency calculations has to do with the calculation of T_{max} by applying equation (6). With 150 W/m^2 incident global solar radiation, for a vertical surface, we would obtain that $T_{max} = T_{out} + 7.8^{\circ}C$, while for a roof $T_{max} = T_{out} + 7.8 - 4^{\circ}C = T_{out} + 3.8^{\circ}C$. In cold days, the wet bulb temperature is very close to the ambient air temperature, so from equation (7), we can say that $T_{min} = T_{wet-bulb} \approx T_{out}$. Thus, the denominator $T_{max} - T_{min}$ of equations (4) and (5) becomes very small and makes the calculation of the cooling and heating efficiencies unstable and uncertain for the instants of time where the incident solar radiation is below 150 W/m^2. For example, for cold winter days, when evaluating the efficiency of a green roof, the term $T_{max} - T_{min} \approx 3.8^{\circ}C$ for an incident solar radiation of 150 W/m^2, an error of 0.5 °C in the temperature differences of the numerator will represent a 13% error in the efficiency calculation. Note that, for sunny clear days, > 90% of the incident solar energy occurs when solar incident radiation is over 150 W/m^2. Thus, the efficiency value represents how well or badly we evacuate or capture the main part of the incident solar radiation thanks to the selected skin solution.

The heating and cooling efficiencies of the skin components must be calculated experimentally on completely clear sunny days. Since the same skin component's heating or cooling efficiency should be similar if

the skin solution is tested in different completely clear sunny days, the repeatability of the obtained efficiency values is crucial. When global solar irradiation is over 150 W/m^2 and with a frequency of at least 10 min, the instantaneous efficiencies must be calculated and all those values must be averaged to obtain a daily averaged efficiency value.

To check the repeatability of those daily values on a complex skin solution, a MLW has been tested for a whole year in a well-controlled experimental facility. All the completely clear sunny days have been identified for two periods, the hot season and the cold season. The efficiency values of all those days have been calculated and the spread (standard deviation) on each season and the similarity of the efficiency between seasons have also been analysed by comparing the mean of all those daily efficiencies.

2.2. Proving the conduction heat transfer is negligible in the energy balance of a building envelope component's outermost surface during sunny hours

The method presented in section 2.1, requires validating this strong assumption: the conduction heat transfer is negligible in the energy balance of a building envelope component's outermost surface during sunny hours. The assumption must be valid for a wide range of wall solutions with different thermal transmittance and thermal inertia and for hot and cold climates. This validation is going to be done by simulating a series of four wall solutions under three different climate conditions and for a whole year. Then, the weight of the conduction heat transfer in the energy balance of the outermost surface layer of the wall is going to be analysed for all cases. The well-known TRNSYS simulation software have been selected to perform this analysis.

Considering a general n layer building component, as shown in Fig. 1, the energy balance in the control volume representing a general skin solution would be calculated by equation (10) (assuming all heat fluxes to be positive in the direction towards the control volume):

$$G_{sol}\cdot\alpha + q_{conv} + q_{rad,lw,surr} + q_{rad,lw,sky} + q_{evap} + q_{cond} = 0 \quad \left[\mathrm{W/m^2}\right] \qquad (10)$$

where: G_{sol} is the incident global solar radiation on the surface [W/m^2]; α is the absorptivity of the surface for solar radiation; q_{conv} is the convection heat transfer [W/m^2]; $q_{rad,\ lw,\ surr}$ is the long-wave radiation exchange between the outer surface and the surroundings [W/m^2]; $q_{rad,\ lw,\ sky}$ is the long-wave radiation exchange between the outer surface and the sky [W/m^2]; q_{evap} is the evaporation heat transfer [W/m^2] (if it exists, not shown in Fig. 1); and q_{cond} is the conduction heat transfer [W/m^2].

When analysing building components with and without vertical greeneries, the difference is the presence or absence of the term q_{evap}. In a general case, for façades without VGS, the weight of the term q_{cond} in the energy balance would be greater than if a VGS façade with q_{evap} term were considered. Therefore, this study aims to demonstrate that the q_{cond} heat exchange is negligible compared to the sum of the rest of the heat exchanges that occur in the outermost surface of a building envelope component over a whole year for sunny hours. For this reason, a generic analysis will be carried out for a case without the term q_{evap}, which will give a higher weight of the q_{cond} term value.

Therefore, the validation will be performed for the extreme case, where the weight of the term q_{cond} is maximum. Consequently, the assumption that the conduction heat transfer is negligible will also be valid for the cases with a different skin solution in which extra heat transfer mechanisms appear in the outermost layer, such as q_{evap} or q_{elec}; in these cases, the weight of q_{cond} would be lower.

2.2.1. Reference building description

Using a simple space, in which the phenomena of interest can be separated from the rest of the phenomena that occur in a real building, is an approach that has already been used by other authors [48,49].

A space formed by a square floor of 4 m each side (16 m^2 of floor) and 2.5 m high (from now on reference building) has been chosen for this study. As shown in Fig. (4.a), the building has been oriented parallel to the cardinal axes, the wall oriented to the south being the object of analysis (in red in Fig. (4.a)). For the sake of simplicity, the above-mentioned wall has been considered to be formed by a single homogeneous material. Depending on the case of study, the physical properties have been changed in order to analyse the effect of the thermal conductivity and thermal inertia.

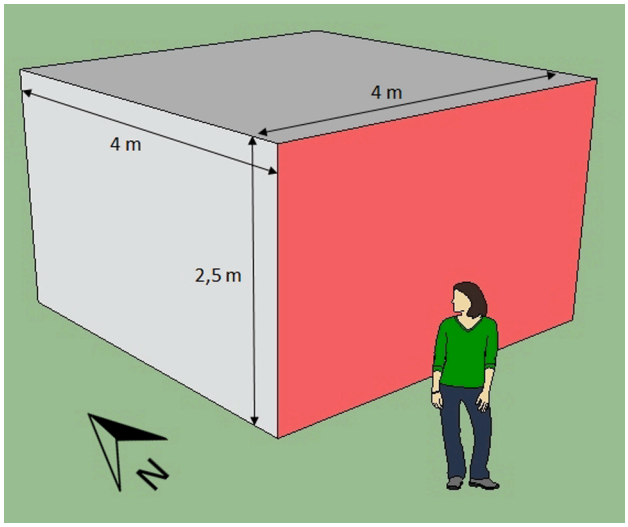

Fig. 4a. Dimensions and orientation of the reference building.

In order to be able to identify the effects related to the variation of the physical properties of the wall, some simplifications have been made. These simplifications have been used to make the analysis of the results easier, thus facilitating the comparison between the walls. Some of these simplifications may involve a certain "idealisation" of the behaviour of the building. The assumed simplifications are as follows:

- There is no conduction heat transfer through the building envelope except for the wall under study (the south wall). Therefore, the rest of the vertical walls, ceiling and floor have been considered adiabatic.
- The presence of glazed surfaces is not considered. In order to facilitate the calculation of the radiation exchanges inside the premises, it has been assumed that there is no semi-transparent element that allows the entry of solar radiation into the reference building.
- In the same way, no internal gains due to occupation, equipment or lighting have been considered.
- The building is considered airtight, so there will be no energy demand due to the external air inlet (voluntary by ventilation or involuntary by infiltration) to the interior of the reference building. Considering that, except for the object wall, the rest of the walls are adiabatic, it can be concluded that the entire energy demand is related exclusively to the characteristics of the object wall.
- The effects of shading produced by constructive elements, remote objects or other buildings are not considered.

The effects of other types of parameter, such as the geometry of the building or its orientation, have not been considered. In order to narrow down the number of cases, variations in the orientation, appearance or compactness of the building have not been considered.

2.2.2. Parameters used in the simulations

With the aim of analysing how the q_{cond} term weight varies with the climate conditions, the analyses carried out throughout this study have considered the reference building located in various locations. These locations have been chosen as representative of 3 climatic zones established in the Spanish Technical Building Code CTE [45]. The CTE is the

Table 1
The seasonal averaged climatic characteristics in the different locations.

G solar, south vertical [W/m^2]	Outdoor temperature [°C]	Humidity [%]	Season	Location
121.92	17.73	75.34	Spring	Almería
126.64	25.14	71.47	Summer	
153.92	18.10	71.65	Autumn	
167.70	13.81	71.89	Winter	
111.06	14.29	72.42	Spring	Bilbao
115.67	19.90	73.70	Summer	
106.53	13.03	74.47	Autumn	
110.38	7.95	75.20	Winter	
120.27	10.33	73.10	Spring	Burgos
136.05	17.64	65.59	Summer	
120.29	8.02	81.55	Autumn	
127.98	3.50	81.71	Winter	

regulatory framework that establishes the requirements to be met by buildings in relation to basic safety and habitability requirements.

The climate selection has been made with the aim of including the most significant ones for the q_{cond} term weight analysis proposed in this study. A location with severe summer conditions (Almería), another one with severe winter conditions (Burgos), and finally a zone with moderate climatic characteristics (Bilbao), have been selected. The climatic zones they belong to, according to the Spanish CTE regulations, are A4, E1 and C1, respectively [45]. The season averaged global vertical south solar radiation, outdoor temperature and relative humidity of the selected locations can be seen in Table 1.

The weather data used in the simulation as input are those corresponding to the meteorological year type of the aforementioned localities. These data have been collected using the software Meteonorm [50].

The heating and air conditioning system in the building is assumed to be powerful enough to keep the internal temperature between 20 °C and 26 °C at any time. In order to facilitate the analysis, the system is assumed to be 100% convective, transmitting all the power to the air, without heat radiation exchange with the building's walls. The initial enclosure temperature values have been assumed to be equal to 20 °C. The selection of this initial value has no effect on the results, because the simulations have been carried out considering a two year period, selecting the values of the second year as the results.

The convection coefficients, both exterior and interior, have been assumed constant throughout the simulation. The values adopted have been the ones defined in the standard UNE EN ISO 6946 [51]. The pure convection coefficient values adopted for the simulations are presented in Table 2 (long wave radiation effect not considered within them).

The absorptivity value used for the short-wave radiation was 0.7 and the emissivity value used for the long-wave radiation exchange was 0.9.

The TRNSYS model is used to calculate the interior and exterior surface temperatures of the south wall for a whole year of each analysed case. Then, these temperature values have been used as input variables for the code in finite differences resolved with MATLAB, where the conduction heat flows have been calculated for the outermost surface. The modules used in TRNSYS were the following: Type 109-TMY2 - Weather Data Reading and Processing, Type 33e – Psychrometrics, Type 69b - Sky Temperature, Type 56b - Multi-zone building, Type 25b – Printer, Type 28b – Printer and Type 65d - Online plotter. The TRNSYS model flow diagram is illustrated in Fig. 4b.

Table 2
Convection coefficients adopted for the simulations.

Heat flow direction	$h_{conv,in}$ [W/(m^{2}K)]	$h_{conv,out}$ [W/(m^{2}K)]
Horizontal	2.9	23
Vertical upward	5.8	23
Vertical downward	0.81	23

For the MATLAB code, the chosen time frame was $\Delta t = 60$ s and the distance between nodes $\Delta x = 1$ cm (using smaller Δt and Δx did not produce any variation on the obtained results). The different heat flows (in absolute values) have been accumulated in annual values and used in the analysis.

The reference building described above, with the considerations previously commented, provided the necessary information to address the cases. The object wall (the south wall) was defined as a homogeneous enclosure 30 cm thick. Twelve cases, formed by the combination of 2 thermal transmittance, 2 thermal inertia and 3 climates, have been selected. It can be observed that the selected transmittance and inertia values consider high and low limiting values commonly used in the construction sector.

Each case has been appointed with a code formed by the letter W plus a number (1, 2, 3 or 4), depending on the thermal transmittance and inertia of the wall, plus a letter (A, C or E) corresponding to the climatic zone of the chosen location. The considered values for the climate-inertia-thermal transmittance combinations are presented in Table 3.

2.2.3. Theoretical approach to estimate the outermost surface heat fluxes

As the main purpose of this simulation is to quantify and compare the weights of the different energy exchanges in the outer surface of the object wall, a detailed schematic of all energy exchanges involved is shown in Fig. 5. With reference to the direction of the energy flows in Fig. 5, the outer surface energy balance is shown in equation (11) (represented as heat fluxes).

$$q_{cond,surf-out} = q_{conv,out} - q_{rad,sw,out} + q_{rad,lw,sky} + q_{rad,lw,surr} \quad \left[W/m^2\right] \tag{11}$$

The thermal behaviour of the wall in its outermost surface is evaluated considering all the mechanisms involved individually (conduction, short-wave solar radiation, long-wave exchange with the surroundings and with the sky, and convection with outside ambient air).

This study aims to prove that the energy balance that occurs in the outermost layer of the envelope can be simplified, considering the mechanism of heat conduction through it to be negligible, since its value is negligible when compared to the sum of the values of short-wave radiation, long-wave radiation, and convective heat exchanges that occur in it. This assumption would allow us to accurately estimate the $T_{surf\text{-}out}$ value, applying only the energy balance in the building envelope outermost surface without considering the q_{cond} term in the energy balance when solar radiation is present.

2.3. Description of the PASLINK test cell

The method presented in section 2.1 is going to be tested for a specific skin solution: a modular living wall (MLW). This MLW skin solution is going to be installed on the outermost surface of a base wall and tested for a whole year under real weather conditions under the PASLINK methodology. The PASLINK test cell is a well-insulated structure that consists of two spaces. An area of 5.0 × 2.7 × 2.7 m^3 called the "test room", and an adjoining area called the "service room". The south façade (and roof in some PASLINK test cell types) of the test room is interchangeable, so it is possible to test different building components (walls or roofs). Fig. 6 shows a scheme of a PASLINK test cell.

In the PASLINK cells, heat transfer through the enclosure to the test room is accurately measured or controlled. Thus, all the heat passing through the element (to be tested) can be properly evaluated. Calibration and test procedures were also developed and tested during the PASLINK project and these are fully developed in [53,54]. All the actions carried out in setting up the PASLINK test cells of the Laboratory for the Quality Control in Buildings (LCCE laboratory) of the Basque Government, where the tests of this work were carried out, have been performed to fulfil all the requirements described in these PASLINK documents.

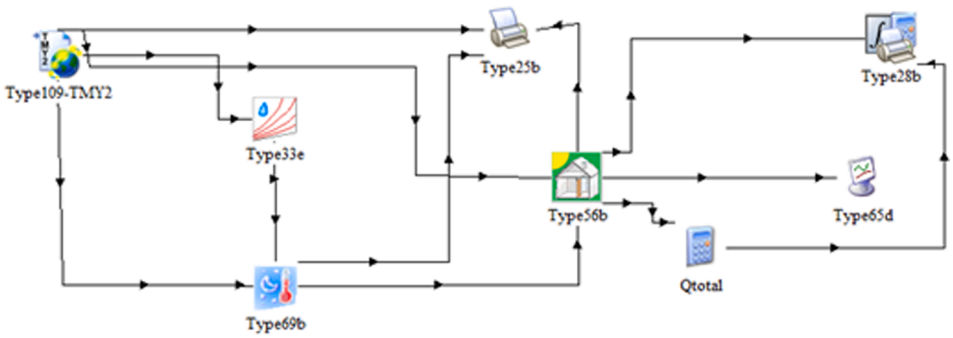

Fig. 4b. TRNYS model flow chart.

Table 3
The characteristics of the 12 analysed cases.

Code	Transmittance U [W/(m^{2}K)]	Volumetric heat capacity C [MJ/(m^{3}K)]*	Location
W1A	0.13	0.50	Almería
W2A	0.13	4.00	
W3A	1.30	0.50	
W4A	1.30	4.00	
W1C	0.13	0.50	Bilbao
W2C	0.13	4.00	
W3C	1.30	0.50	
W4C	1.30	4.00	
W1E	0.13	0.50	Burgos
W2E	0.13	4.00	
W3E	1.30	0.50	
W4E	1.30	4.00	

* The wall's heat capacity per wall m^2 would be obtained by multiplying the volumetric heat capacity by the thickness of the wall (0.3 m).

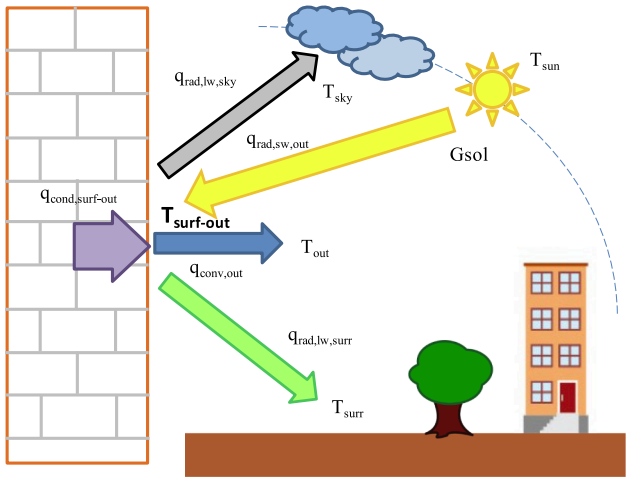

Fig. 5. Outer surface energy exchanges.

2.4. Description of the Modular living wall (MLW) test sample

The component to be tested and analysed in this study is a base wall with a MLW skin solution installed on the South face of a PASLINK test cell. The base wall section schematic is presented in Fig. 2, it consists of a double-sided vertical enclosure without glazing made, from inside to outside, in the following materials: cement mortar (1.5 cm), double hollow brick (32 cm × 14 cm × 6.4 cm thick), unventilated air chamber (10 cm) and face brick (22.8 cm × 49 cm × 10.5 cm thick). The dimensions of the tested sample were 2.7 × 2.7 m (sample area 7.3 m^2), with the thermal transmittance of the base wall being 0.77 W/(m^2 K).

With reference to the MLW skin solution shown in Fig. 7, it consists of an air chamber (5 cm), a layer formed by a metallic substructure anchoring the MLW to the base wall, an outside layer of a pre-cultivated plant module (8 cm) [55] and, finally, an irrigation and drainage system. The pre-cultivated modules in the outside layer are made of recycled polyethylene 60 cm wide by 40 cm high and 8 cm thick. The modules do not contain any polyvinyl chloride (PVC) material, so they are suitable for sustainable construction. Due to their dimensions, they provide a sufficiently large water reserve to minimize the risks of a lack of water.

The metallic substructure supporting the modules is made of a vertical stainless steel frame Fig. 7 that acts as an anchoring element where the modules are placed. The four polyethylene hooks located at the back of the plant modules enable the anchoring to the vertical steel structure profiles. This structure does not allow the vegetated modules to be extracted perpendicularly from the wall. In this way, module thefts are avoided.

Four entrances for the drippers are placed in the upper part of the modules, while the two drainage exits are located at the bottom. Modules are hermetically sealed so that no water is poured onto the inside of the plant façade. In this way, there is no need for prior sealing work on the façade. The façade is covered 100 per cent by the modules, thus avoiding additional work to finish the wall.

The irrigation system used in the test is automatic and responds to the fertigation techniques used in hydroponic crops. The nutrient solution is distributed in small quantities in localised areas by self-compensating droppers, so that the plant growth can be controlled by adjusting the nutrient solution and, at the same time, reducing the need for irrigation water. The system is complemented by filtration elements, irrigation control and a pump to raise and distribute the water throughout the MLW. An evergreen shrub (*Helichrysum italicum)* was selected in this test to guarantee the uniformity of the MLW.

2.5. Experimental testing and instrumentation

The PASLINK test cell used in this study is located in the facilities of the Laboratory for the Quality Control in Buildings of The Basque Government (LCCE), (latitude: 42°51́N, longitude 2°41́W) in Vitoria - Gasteiz, Spain. The experiments were carried out between January and December 2014.

The standard sensors for a PASLINK test cell were used in this test and registered at 1 min interval and then averaged to 10 min intervals [56]. However, to apply the method proposed in section 2.1, only a few of those sensors are needed: the outermost surface temperature of layer 4 (see Fig. 2) in four locations (see also Fig. (7.c)), the outdoor air temperature, the outdoor air relative humidity and the global vertical south solar radiation incident on the MLW. Thus, the description of the sensors used in this research are commented on here.

The temperature of the $T_{surf-out}$ layer of Fig. 2 was measured with four platinum thermoresistances Pt100 (measurement accuracy ± 0.1 °C), the average of those four signals has been considered for this analysis as the $T_{surf-out}$. In front of the MLW the outdoor air temperature was measured with a platinum thermoresistance Pt100 (measurement

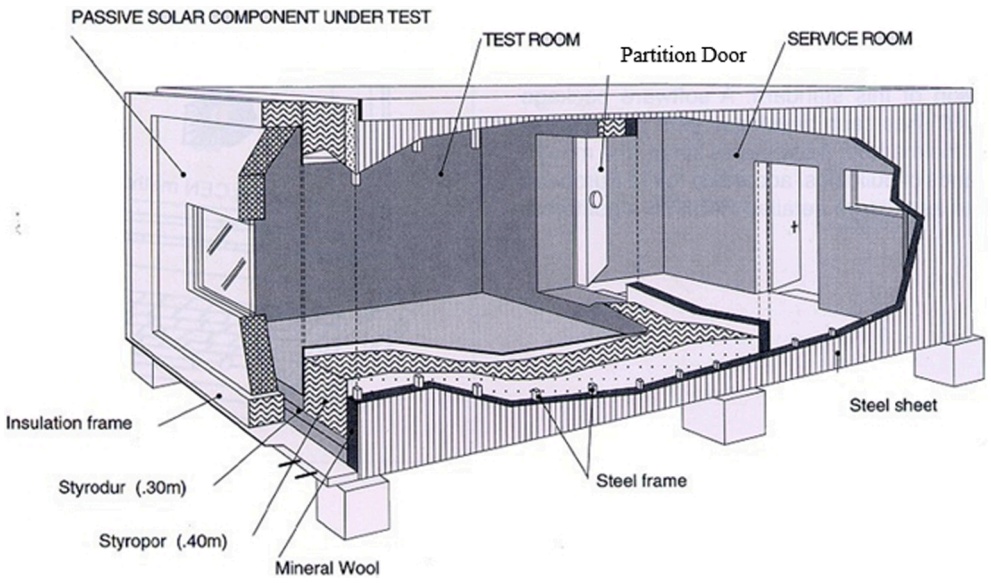

Fig. 6. General structure of the PASLINK test cell [52]. NOTE: the component under test in this figure is a general passive component, it is not the MLW tested within this research.

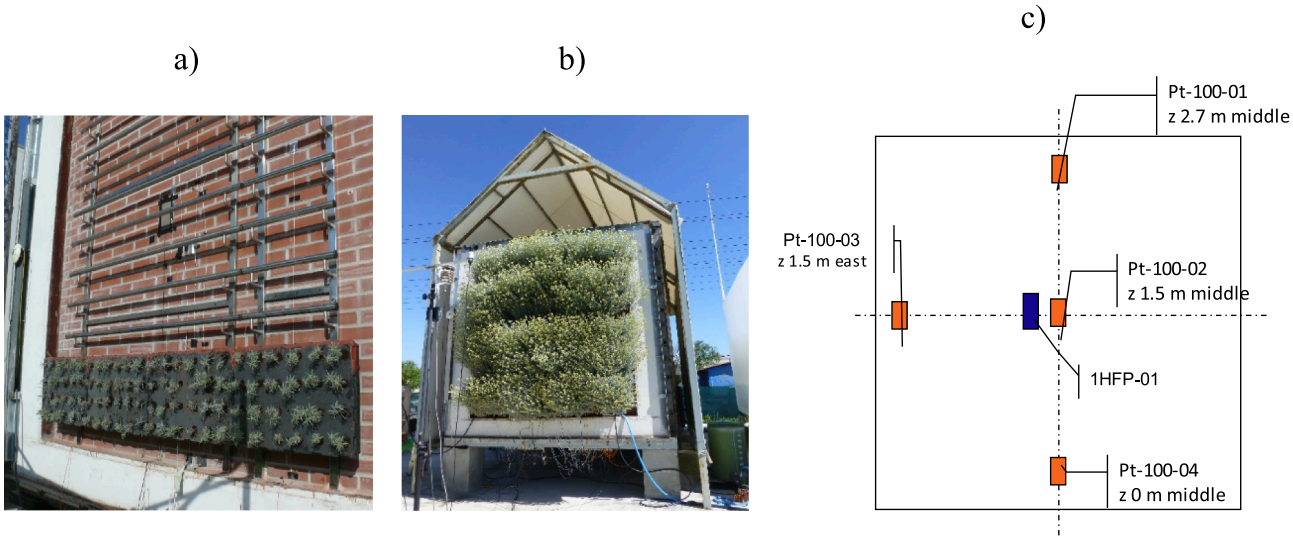

Fig. 7. a) Details and measurement devices in the tested base wall outermost surface installed in the PASLINK test cell at LCCE (plants still not grown) b) the MLW front view during the test (once the plants has been grown). c) Front view representation of the layer $T_{surf\text{-}out}$ of Fig. 2 where the position of the surface temperature sensors used in this research can be seen. NOTE: there was also a heat flux sensor (1HFP-01), but has not been used in this research.

accuracy ± 0.1 °C), protected against radiation and mechanically ventilated. The relative humidity was measured in front of the MLW with an AHLBORN FHA 646 E1 sensor (measurement accuracy ± 2%). Finally, the vertical global solar radiation incident in the plane of the tested MLW was recorded using a Kipp&Zonen CM11-P pyranometer (measurement accuracy ± 3%). All the sensors were calibrated before installation in the experimental setup and were connected to the main data acquisition unit Agilent 34970A.

3. Results and discussion

3.1. Results of the outermost surface heat fluxes weight analysis

The cases analysed to find out what happens in the energy balance of the outermost surface of the walls correspond to the 3 climates × 2 inertia × 2 thermal transmittances combinations presented in section 2.2. The use of these cases gives a general overview of the weight the conduction heat flow has in the outermost surface of a general building component compared to the rest of the heat flows towards the ambient.

The analysis of the heat flows is based on the relative weight of each mechanism in the total energy balance of the outermost surface of the wall, as well as the influence of the different parameters (inertia, climate and thermal transmittance) on the values of the corresponding flows.

Fig. 8 shows the accumulated annual energy balance of the heat fluxes that make up equation (11) for all the hours when the solar radiation values are>150 W/m^2. For clarity, in Fig. 8, the long wave radiation heat exchanges with the sky and surroundings have been grouped as follows:.$q_{rad,lw} = q_{rad,lw,sky} + q_{rad,lw,surr}$

In the first case study (1), in which both, the thermal transmittance (0.13 W/(m^2 K)) and the heat capacity (0.50 MJ/(m^3 K)) are low for the three different climates (A, C, E), the percentage of q_{cond} is lowest (below 2% for the three climates), q_{conv} between 29 and 32%, $q_{rad,\ sw}$ between 53 and 55% and $q_{\ rad,\ lw}$ about 14% of the total annual energy balance (during sunny hours). In case (2), where the heat capacity is increased

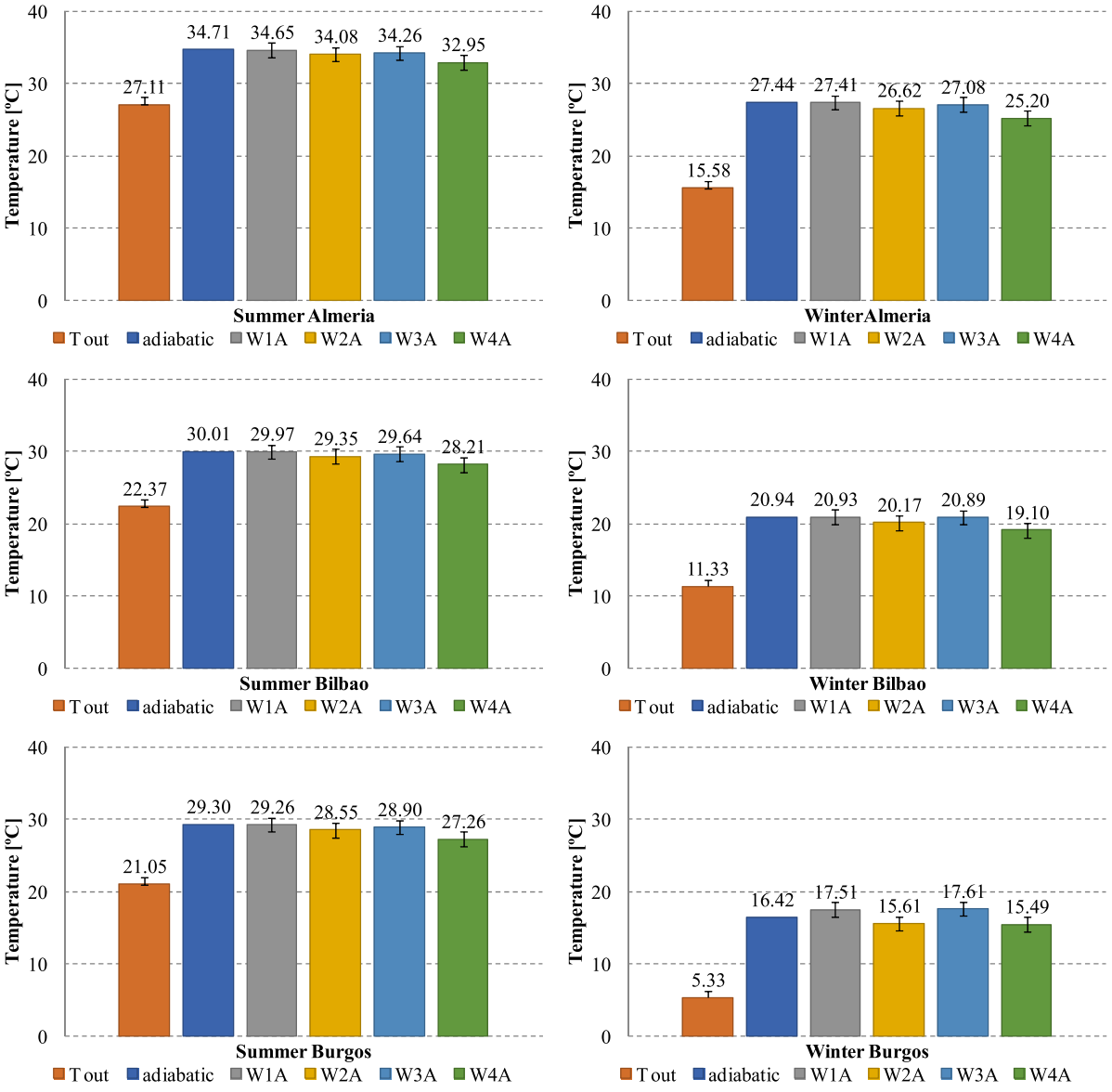

Fig. 8. Outermost surface energy annual balance percentages for the considered climate-inertia-thermal transmittance combinations considering all the sunny hours with $G_{sol} > 150$ W/m^2.

(4 MJ/(m^3 K)) and the thermal transmittance is kept low (0.13 W/(m^2 K)), the values of all the q_{cond} term is approximately doubled compared to case (1). The values show that the q_{cond} for the three climates remains similar at 4%. In case (3), where the thermal transmittance is increased (1.30 W/(m^2 K) and the heat capacity remains low (0.50 MJ/(m^3 K)) the q_{cond} is approximately triplicated compared to case (1) and represents about the 6% for the three climates studied. In the last case (4), where both the thermal transmittance (1.30 W/(m^2 K)) and the heat capacity are high (4 MJ/(m^3 K), the weight of the conduction heat flows (q_{cond}) increases to about 12–13% (this is about six times the weight of case (1)). The latter case is the most unrealistic, but it shows that only in the cases of walls with high inertia and high thermal transmittance does the weight of the conduction heat flow in the outermost surface energy balance have a not negligible weight.

The previous analysis show that it is possible to neglect the q_{cond} term in the energy balance of usual wall compositions to calculate the $T_{surf\text{-}out}$ value during sunny hours. Therefore, it is possible to carry out the heat exchange balance on the outermost surface of the building component without considering the term q_{cond}.

Furthermore, when performing the analysis of a VGS or a GR, as stated in equation (10), the term q_{evap} associated with this type of skin solution must be taken into account. In this simulation study, a wall where the q_{evap} effect does not exit has been evaluated. In this way, the extreme case where the weight of the term q_{cond} is maximum, has been analysed and validated. In other words, Fig. 8 represents the maximum values that the q_{cond} term could present on the analysed wall, which would be reduced if a new heat transfer mechanism were to be incorporated in the outermost surface, such as q_{evap}.

The obtained $T_{surf\text{-}out}$ values obtained for the 12 different scenarios (3 climates × 2 inertia × 2 thermal transmittances) and for a hypothetical perfectly, adiabatic wall have also been analysed. Such season averaged temperature values have been compared with the season averaged outdoors air temperature, for the hours where the solar radiation values are higher than 150 W/m^2.

In Fig. 9, the outdoor air temperature and the outer surface temperature for the summer and winter periods and for the considered 12 cases are presented only considering all the sunny hours with $G_{sol} > 150$ W/m^2. The season averaged outdoor air temperature values differ

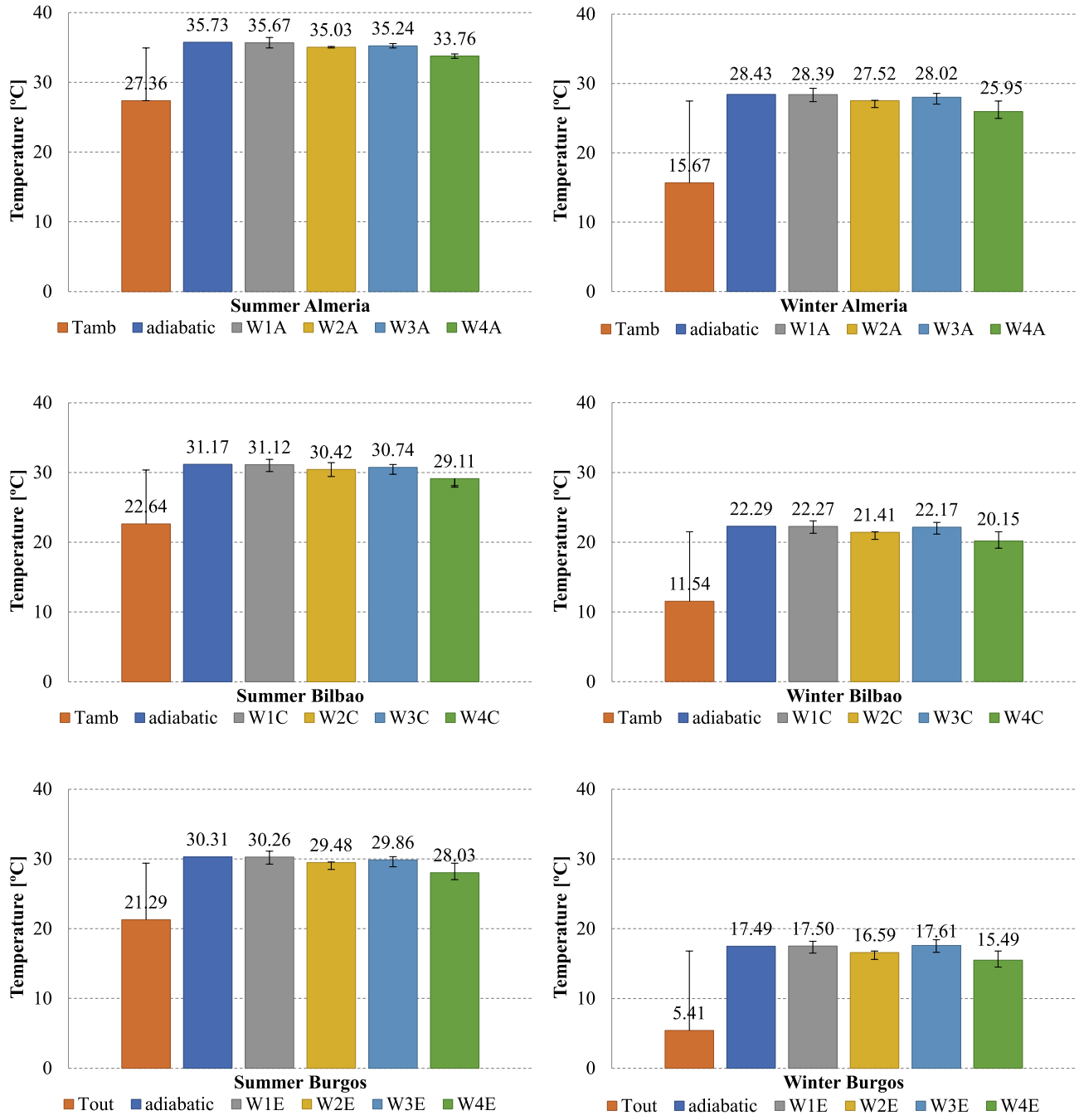

Fig. 9. Outdoor air temperature and outer surface temperatures for the considered climate-inertia-thermal transmittance combinations.

greatly from the calculated exterior surface temperatures. The inequality that occurs with the ambient temperature is greater for winter cases.

The results presented in Fig. 9 reveal that, in the periods of solar radiation (>150 W/m^2), the calculated temperature of the outermost surface, in all the study cases, differs between the different construction solutions only by ± 1–2 °C. The lower limit of the temperatures always corresponds to the combination of high inertia and high thermal transmittance (W4); logically, this is the case where the q_{cond} term weight is maximum. On the other hand, the upper limit is established by the façade considered adiabatic.

Given that the outdoor air temperature in the degree-day method is currently used to calculate the demand for cooling and heating, it is worth noting that, performing this calculation with the outermost surface temperature ($T_{surf\text{-}out}$) calculated using the proposed efficiency methodology, it is much closer to the real temperature of the outermost façade surface. Therefore, the use of this method would make the degree-day method much more precise and the heating demands would not be overestimated and cooling demands underestimated.

3.2. *Calculation of the cooling efficiency throughout a whole year for a MLW*

After validating in the previous section 3.1 the strong assumption about the negligible weight the conduction heat flow has in the energy balance of the outermost surface of a building component, in this section, the proposed method to estimate the heating and cooling solar efficiency is applied to a MLW. In order to evaluate the cooling efficiency

of the tested MLW, the minutely acquired data have been averaged every 10 min and collected in a file containing all the measurements over one year (2014). The three temperatures (T_{max}; T_{min}; $T_{surf\text{-}out}$) have been plotted in two periods as examples. The first period lasts from August 5th to 15th and the second from March 7th to 17th.

- $T_{surf\text{-}out}$ is directly measured on the tested sample outermost surface;
- T_{max} is calculated using equation (6) with the measured outdoor air temperature and the measured global solar radiation incident on the tested sample;
- T_{min} is calculated using equation (7) with the measured outdoor air temperature and the measured outdoors air relative humidity.

It is possible to graphically see the meaning of the cooling efficiency as the ratio between ($T_{max} - T_{surf\text{-}out}$) and ($T_{max} - T_{min}$). It is clear that the cooling efficiency will reach its maximum value when the temperature of the exterior layer is as close as possible to the ambient wet bulb temperature, which is identified as the best possible condition for summer and the worst for winter.

The tests have been conducted in the PASLINK test site located in Vitoria-Gasteiz. Even if there is no official heating period established by the authorities in this area, the heating season starts at the beginning of autumn and finishes at the beginning of spring. Thus, even if the results of the efficiency are very similar throughout the whole year, the analysis have been done dividing the year into two periods: the cold season considers autumn and winter (the period when the heating systems are usually ON), while the hot season considers spring and summer (the period when the heating systems are usually OFF).

3.2.1. *Cooling efficiency during hot season (spring and summer).*

A representative period of the cooling efficiency results in summer's hottest days is presented in Fig. 10, in which the measured incident global solar radiation, the measured outermost surface temperature and calculated T_{max} and T_{min} temperatures, together with the estimated cooling efficiency, are shown together. During the testing days, solar radiation started at 06:00 h and faded away at 18:00 h (UTC hour). Clear days can be identified by an almost regular bell shape (i.e., 5th, 6th). The cloudy days (i.e., 7th to 15th) had a very irregular behaviour of the solar radiation due to passing clouds. This indicates that many days did not have completely clear skies during the testing period.

During some of the days, the air temperature increased by midday up to 30 °C (7th, 8th, 9th and 10th), although the temperature of the exterior surface never reached values higher than 25 °C. During the sunny hours, the temperature of the outermost surface is always lower than the temperature of the air and very close to the wet bulb temperature. However, during the hours in which there is no solar radiation, from 18:00 to 06:00, the temperature of the outermost surface is above the temperature of the air (probably maintained thanks to the green cover).

A detailed cooling efficiency curve is visible in Fig. 11. The cooling efficiency curve usually starts with a slight peak in the early hours of the morning, when the MLW panels are coldest due to early morning irrigation and the thermal inertia effect of the colder night. Then, as it stabilises, it draws a flat curve during the central hours of the day when the solar radiation is high. Finally, in the afternoon, as solar radiation disappears, the cooling efficiency slightly decreases, reaching its minimum at the moment when solar radiation disappears, which coincides with the moment when the plant panels are drying out.

In the case of Fig. 11, the early morning irregular peaks in the cooling efficiency curve are not only caused by the irrigation that occurs in the early morning combined with the inertia of the night-time temperature, but also have to do with the early morning cloud passing effect that decreases the incident solar radiation to about 200 W/m^2 and makes the efficiency calculation more unstable. As stated in the methodology section, this is why the efficiency values are only calculated for cases

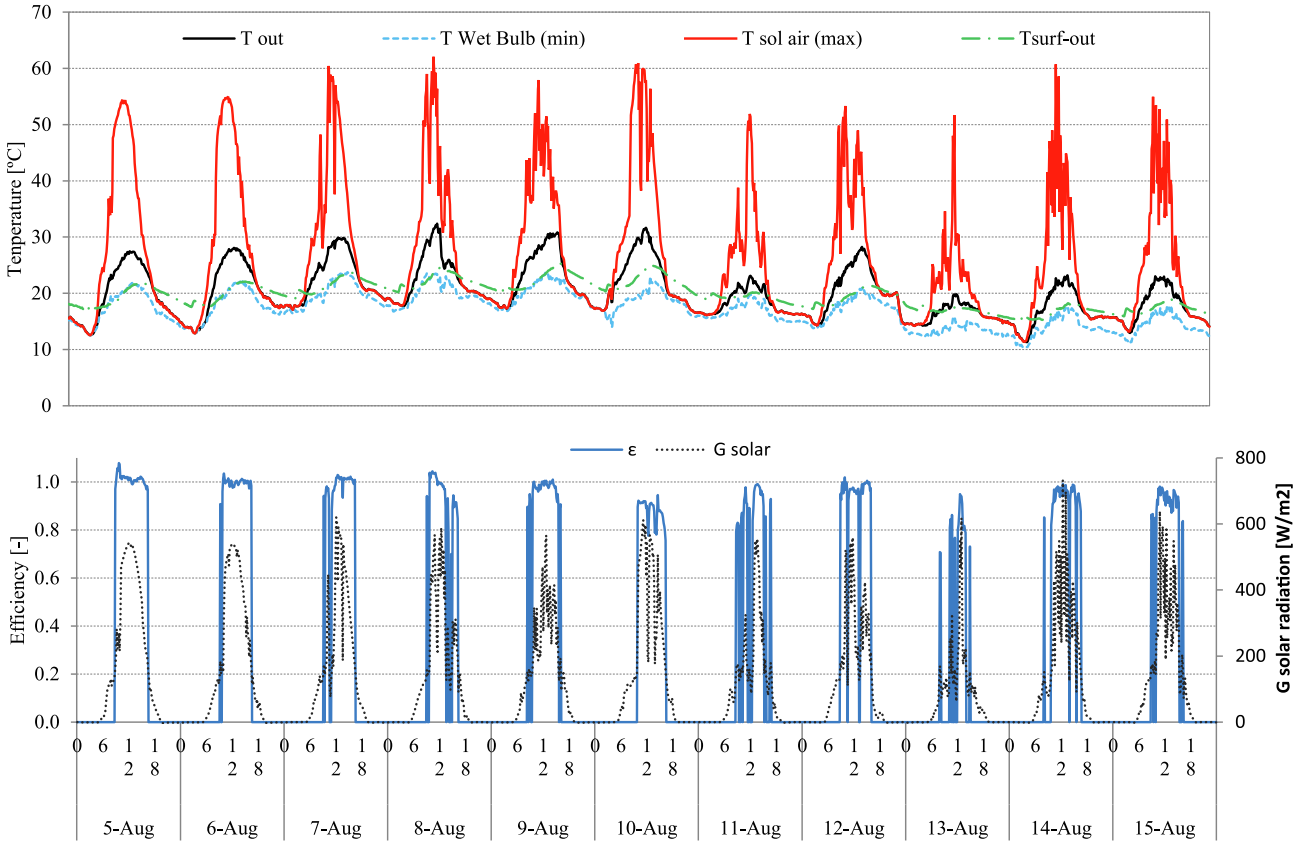

Fig. 10. Evaluation of temperatures, cooling efficiency and the incident global solar radiation data, registered from August 5th to 15th. (Sharp fluctuations in solar radiation are due to cloud movement).

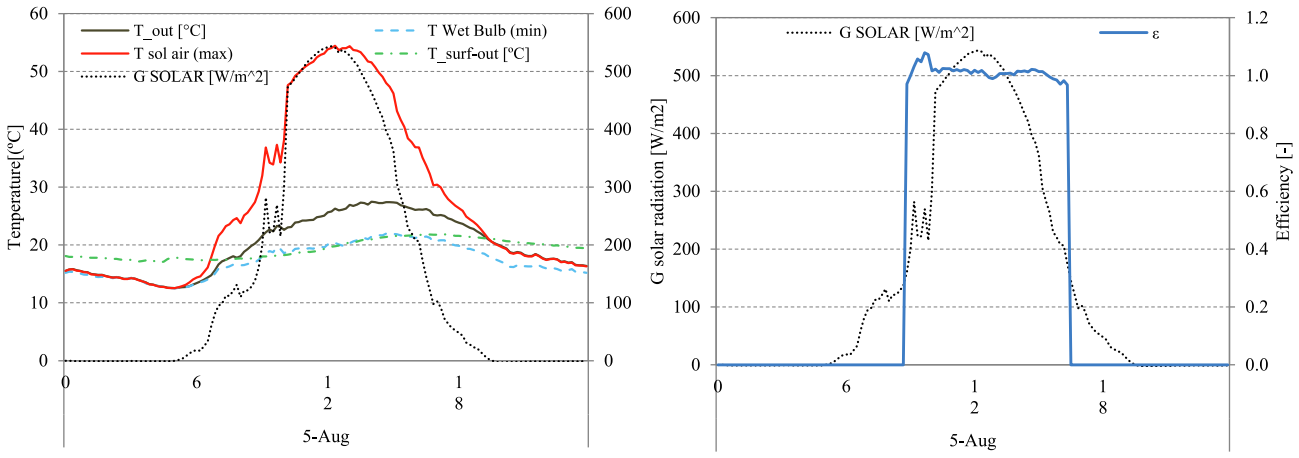

Fig. 11. Detail of the profile of temperatures, incident global solar radiation and cooling efficiency for the 5th August (summertime).

where the incident solar radiation is over 150 W/m^2. The cooling efficiency in this type of MLW is not influenced by rainfall, as water is always available to the plants in the growing layer through the irrigation system.

On the other hand, the presence of clouds throughout the day causes fluctuations in the solar radiation curve, which are reflected in the peaks and irregularities of the thermal efficiency values. For this reason, when defining the efficiency, it is necessary for the efficiency to be calculated on completely sunny, clear days, while cloudy days are not taken into account.

To analyse the repeatability of the MLW cooling efficiency, it was necessary to calculate the daily cooling efficiency values of all the available clear sunny days. Then, averaging all these daily values of the hot season (from March 20th to September 22nd), a representative value for the cooling efficiency in hot conditions is obtained: $\varepsilon = 0.9076$ [-] (or 90.8% cooling efficiency) with a standard deviation of 0.08 [-]. It is important to note that only the clear days (45 days) are considered in the calculation of this averaged cooling efficiency. Considering the complexity of the heat and mass transfer phenomena occurring in this MLW skin solution, the spread of the obtained experimental cooling efficiencies is considered low.

This MLW skin solution, when properly irrigated, is an extremely adequate system to reduce cooling demands in summer due to heat gains through opaque elements of the building envelope. During sunny hours, it is able to maintain the outermost surface layer of the building component, where it has been installed, very close to the ambient wet

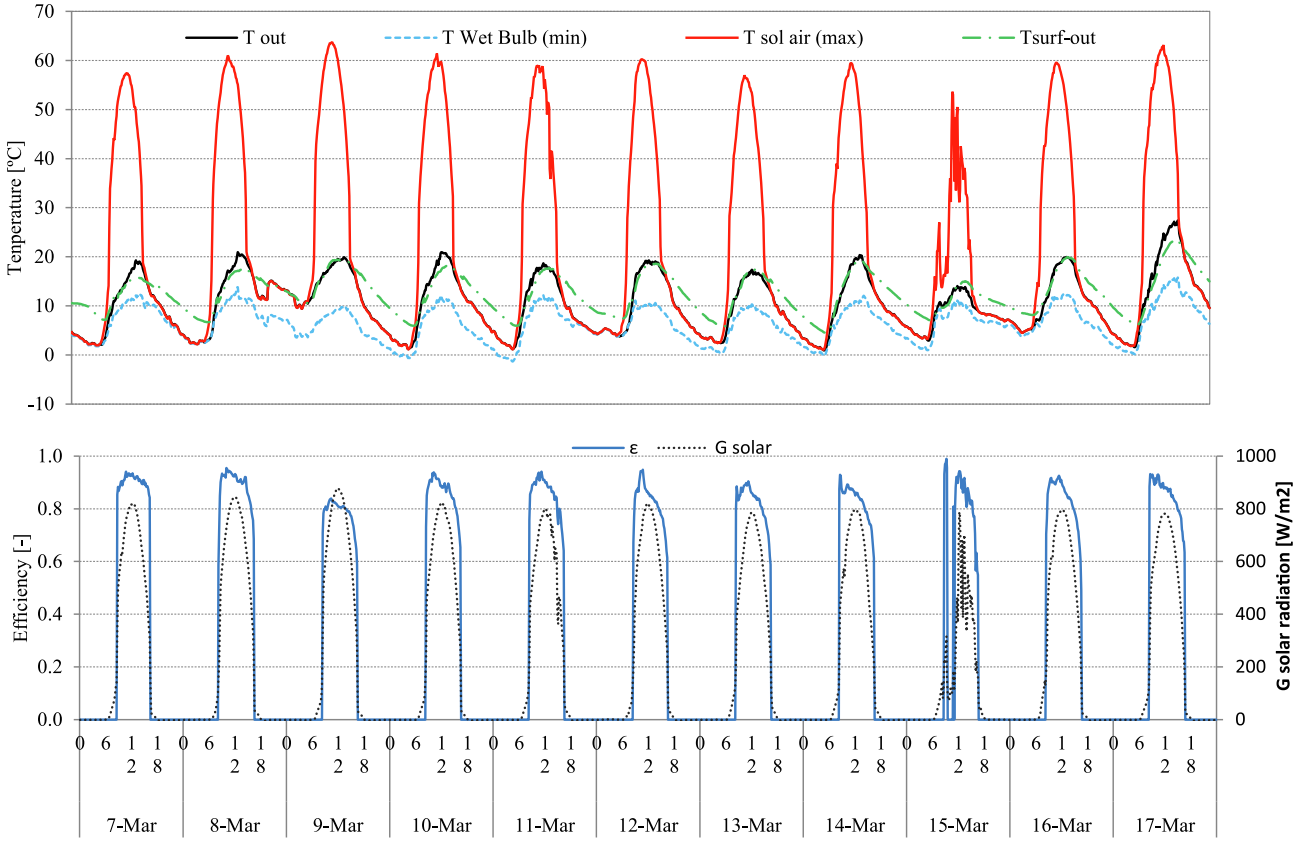

Fig. 12. Evaluation of temperatures, cooling efficiency and the incident global solar radiation data, registered from March 7th to 17th. (Sharp fluctuations in solar radiation are due to cloud movement).

bulb temperature.

3.2.2. Cooling efficiency during cold season (autumn and winter).

As can be seen in Fig. 12, during wintertime, the MLW cooling efficiency values also approach 90%. Again, in order to analyse the repeatability and the spread of the cooling efficiencies during the cold season, the daily cooling efficiencies of clear sunny days have been averaged from 23rd September to 19th March. A mean cooling efficiency value of $\varepsilon = 0.9026$ [-] (or 90.3% cooling efficiency) with a standard deviation of 0.07 [-] has been obtained for the cold season. Both the mean cooling efficiency and the spread of the daily efficiencies are identical to those ones obtained for the hot season. A 90.3% cooling efficiency implies a heating efficiency of just 9.7% for the cold season (see equation (8)). It is important to note that only clear days (28 days) are considered for the calculation of these mean cooling and heating efficiencies. These results indicate that the MLW skin solution behaves identically in both the cold and hot seasons. The latter is crucial, the repeatability between seasons and the low spread of the obtained daily efficiencies should mean that only a short testing period with a few clear sunny days is required in order to obtain reliable heating and cooling efficiency values of skin solutions.

As for the hot season, the temperature of the outdoor air and the outermost surface temperature of the façade are very similar during cold and sunny winter days (see Fig. 12), though $T_{surf\text{-}out}$ is slightly higher than T_{min} (wet bulb temperature). Note that the wet bulb temperature and the air temperature are very close when the air temperatures are low.

Analysing Fig. 13, at about 12:00 h, the maximum possible sol–air temperature according to equation (6) and using the locally measured vertical south global solar radiation, would be 57.1 °C while the outdoor air temperature is 14.7 °C and the wet bulb temperature is 10.7 °C. Since the cooling efficiency at 12:00 h is 92.3%, the outermost surface temperature is only 14.3 °C. The heating efficiency (using equation (5) or equation (8)), would give a value of 7.7%). The day represented in Fig. 13, is a cold sunny winter day that would probably require heating within the building. Having a cooling efficiency of 90% means that the skin solution is generating an undesired cooling effect in the outermost surface of the wall that will generate extra heating demand within the building. For this day, a skin solution that permits to obtain higher temperatures in the outermost surface of the wall would be preferable.

It is evident from the considerations that it is convenient to have a VGS, mainly in hot seasons, since the value of the cooling efficiency represents the goodness of the façade skin solution in decreasing the temperature below the vegetation layer. Due to this, the effect is positive in summer and negative in winter.

The cooling and heating solar efficiency values obtained with the developed method, not only provide a comparable unique efficiency value to understand the performance of this skin solution; they also permit to more accurately obtain the outermost surface temperature of a building component where this skin solution is installed (see equation (9)). These surface temperatures can be used in methods such as the degree-day method to more accurately estimate the heating and/or cooling demands due to the installation of a skin solution in a certain building component as detailed in section 2.1.

4. Conclusions

This research proposes a methodology to experimentally determine the cooling and heating efficiencies of different skin solutions for the opaque elements of a building envelope during sunny hours. Cooling efficiencies of 100% (or 0% heating efficiency) means that the skin solution is able to maintain the outermost surface of the building envelope at the wet bulb temperature of the local weather conditions. This is supposed to be the minimum possible obtainable temperature by passive building skin solutions (T_{min}). On the other hand, heating efficiencies of 100% (or 0% cooling efficiency) means that the skin solution is able to maintain the outermost surface of the building envelope at the sol–air temperature of the local weather conditions. This is supposed to be the maximum possible obtainable temperature by opaque building skin solutions (T_{max}).

These efficiency values give a comparable value of the performance of any skin solution in a unique number. Solutions with high cooling efficiency values would be propitious solutions for reducing the cooling demand in buildings; while skin solutions with high heating efficiencies would be propitious solutions to reduce the heating demand within buildings. However, the definition of the efficiency value needs to prove a strong assumption: that the conduction heat flux has a negligible weight in the energy balance of the outermost surface of a general building component during sunny hours (when the global solar radiation striking the outermost surface is above 150 W/m^2).

The latter strong assumption has been proven and validated by simulating and analysing, over a whole year, the energy balance in the outermost surface of a wall with different thermal inertia and thermal transmittance under three different climate conditions. It has been determined that, independently of the climate, the weight of the heat flux by conduction is negligible (below 6% for walls with common thermal transmittance and thermal inertia values) compared to the sum of the rest of the heat fluxes occurring due to solar radiation gains, losses by convection to the ambient and losses by long wave radiation towards the surroundings and sky. Therefore, it is possible to conclude that the outermost surface temperature of a building component does not depend on the conduction heat flux during sunny hours.

With all this, the developed method to experimentally obtain cooling and heating solar efficiencies of skin solutions has been experimentally

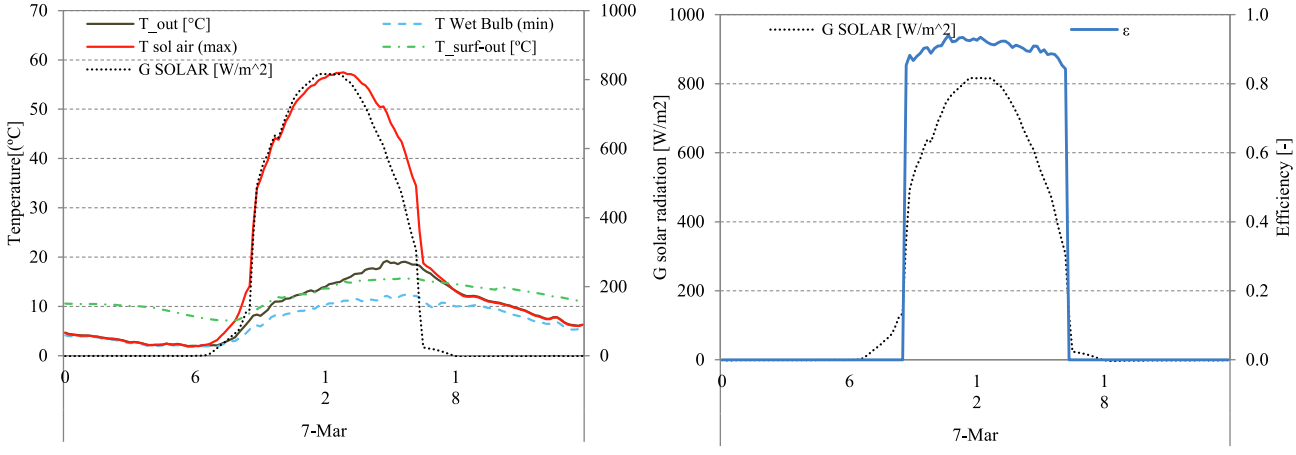

Fig. 13. Detail of the profile of temperatures, incident global solar radiation and cooling efficiency for the 7th of March (wintertime).

tested on a specific skin solution: a Modular Living Wall. A repeatability and spread study of the experimentally obtained cooling efficiency values for clear sunny days was carried out over an entire year on this Modular Living Wall skin solution. The mean cooling efficiency for the hot season and the cold season has been found to be similar; 90.8% and 90.3% respectively. Not only is the mean cooling efficiency similar between seasons, but also the spread of the daily cooling efficiencies has been small and similar for both seasons. This is a clear sign of the repeatability of the proposed method to evaluate the solar behaviour of different skin solutions with a unique efficiency value. These efficiency values make it easy to compare the solar performance of the tested Modular Living Wall with any other skin solution for walls or roofs. From this repeatability study it can be concluded that the testing campaigns required to obtain the heating and cooling solar efficiency values for a certain skin solution would only require a few weeks where few clear sunny days should happen Before the minimum number of required clear sunny days to obtain reliable solar efficiency values can be established, similar repeatability studies as the one performed in this work should be done for other types of skin solutions.

After evaluating the Modular Living Wall's cooling efficiency as a measure to quantify the effect of the vegetation for reducing the outermost surface temperature of the constructive solution; the final conclusion is that the most efficient condition for the Modular Living Wall is in the hot season. The presence of water in summer positively affects the performance of the façade, since it reduces the outermost surface temperature nearly to the wet bulb temperature (this is the minimum possible by passive skin solutions), thus reducing the cooling load of the building. Moreover, during sunny hours the living wall did not allow the façade exterior surface temperature to rise above the air temperature. It is evident from the considerations that it is convenient to have a green façade mainly in hot seasons, since the value of the cooling efficiency represents the goodness of the skin solution in decreasing the temperature of the wall's outermost surface.

On the other hand, for winter, it was noticed that the Modular Living Wall cooling efficiency values approached 90.3% (very similar to the summer cooling efficiency). This is equivalent to saying that the heating efficiency of this skin solution is just 9.7%. This implies that the temperature of the external surface is again very close to the lowest minimum achievable temperature limit, the wet bulb temperature. This means a reduction in the wall's outermost temperature during sunny hours that will lead to a corresponding increase in the heating demand and higher energy costs. In winter, the thermal performance of this skin solution with the irrigation system is not interesting at all due to the cooling effect generated by the evapotranspiration, since it prevents the solar radiation from heating up the outermost surface of the building envelope.

Finally it must be said that, using these cooling or heating efficiencies, it is possible to estimate the outermost surface temperature of a façade very accurately for all the sunny hours over a whole year. This can be done using these single experimental performance parameters and the local weather conditions where it is to be calculated. With this outermost surface temperature, the interior air temperature and with the wall's layers composition, the heat flow through walls with a complex skin solution could be accurately estimated for sunny hours. Note that the degree-day method uses the outdoor air temperature to calculate the cooling and heating demands even in sunny hours where the air temperature and the outermost surface temperature of the wall can differ considerably. Therefore, the use of this solar efficiency methodology could make the degree-day method much more precise in sunny hours, so the thermal demands of the buildings could be better estimated.

Declaration of Competing Interest

The authors declare that they have no known competing financial interests or personal relationships that could have appeared to influence the work reported in this paper.

Acknowledgements

This work was supported by the Spanish Ministry of Science, Innovation and Universities and the European Regional Development Fund (grant number RTI2018-096296-B-C22) through the MONITHERM project 'Investigation of monitoring techniques of occupied buildings for their thermal characterization and methodology to identify their key performance indicators', project reference: RTI2018-096296-B-C22 (MCIU/AEI/FEDER, UE).

Open Access funding provided by University of Basque Country.

References

[1] D. Chiara, Fedrizzi Roberto, B. Elena, H2020 BuildHeat - Retrofit protocols, (2020) 10.5281/zenodo.3734970.
[2] E. Burman, D. Mumovic, J. Kimpian, Towards measurement and verification of energy performance under the framework of the European directive for energy performance of buildings, Energy. 77 (2014) 153–163.
[3] R. Elnaklah, I. Walker, S. Natarajan, Moving to a green building: Indoor environment quality, thermal comfort and health, Building Environment. 191 (2021), 107592.
[4] M. Natarajan, M. Natarajan, M. Rahimi, M. Rahimi, S. Sen, S. Sen, et al., Living wall systems: evaluating life-cycle energy, water and carbon impacts, Urban ecosystems. 18 (1) (2015) 1–11.
[5] M.A. Mir, Green facades and building structures, Delft University of Technology, Delft, 2011.
[6] T. Safikhani, A.M. Abdullah, D.R. Ossen, M. Baharvand, A review of energy characteristic of vertical greenery systems, Renew. Sustain. Energy Rev. 40 (2014) 450–462.
[7] J. Ahern, S. Cilliers, J. Niemelä, The concept of ecosystem services in adaptive urban planning and design: A framework for supporting innovation, Landscape Urban Plann. 125 (2014) 254–259.
[8] P. Wu, Z. Fang, H. Luo, Z. Zheng, K. Zhu, Y. Yang, et al., Comparative analysis of indoor air quality in green office buildings of varying star levels based on the grey method, Build. Environ. 195 (2021), 107690.
[9] M. Viecco, H. Jorquera, A. Sharma, W. Bustamante, H.J.S. Fernando, S. Vera, Green roofs and green walls layouts for improved urban air quality by mitigating particulate matter, Build. Environ. 204 (2021), 108120.
[10] G. Carrus, M. Scopelliti, R. Lafortezza, G. Colangelo, F. Ferrini, F. Salbitano, M. Agrimi, L. Portoghesi, P. Semenzato, G. Sanesi, Go greener, feel better? The positive effects of biodiversity on the well-being of individuals visiting urban and peri-urban green areas, Landscape Urban Planning. 134 (2015) 221–228.
[11] T. Van Renterghem, M. Hornikx, J. Forssen, D. Botteldooren, The potential of building envelope greening to achieve quietness, Build. Environ. 61 (2013) 34–44.
[12] Z. Azkorra, G. Pérez, J. Coma, L.F. Cabeza, S. Bures, J.E. Álvaro, A. Erkoreka, M. Urrestarazu, Evaluation of green walls as a passive acoustic insulation system for buildings, Appl. Acoust. 89 (2015) 46–56.
[13] V. Tsilini, S. Papantoniou, D. Kolokotsa, E. Maria, Urban gardens as a solution to energy poverty and urban heat island, Sustainable Cities and Society. 14 (2015) 323–333.
[14] E.J. Gago, J. Roldan, R. Pacheco-Torres, J. Ordóñez, The city and urban heat islands: A review of strategies to mitigate adverse effects, Renew. Sustain. Energy Rev. 25 (2013) 749–758.
[15] M. Santamouris, K. Pavlou, A. Synnefa, K. Niachou, D. Kolokotsa, Recent progress on passive cooling techniques: Advanced technological developments to improve survivability levels in low-income households, Energy Build. 39 (7) (2007) 859–866.
[16] E. Schroll, J. Lambrinos, T. Righetti, D. Sandrock, The role of vegetation in regulating stormwater runoff from green roofs in a winter rainfall climate, Ecol. Eng. 37 (4) (2011) 595–600.
[17] K. Perini, M. Ottelé, A.L.A. Fraaij, E.M. Haas, R. Raiteri, Vertical greening systems and the effect on air flow and temperature on the building envelope, Build. Environ. 46 (11) (2011) 2287–2294.
[18] E.A. Eumorfopoulou, K.J. Kontoleon, Experimental approach to the contribution of plant-covered walls to the thermal behaviour of building envelopes, Build. Environ. 44 (5) (2009) 1024–1038.
[19] H. Yin, F. Kong, A. Middel, I. Dronova, H. Xu, P. James, Cooling effect of direct green façades during hot summer days: An observational study in Nanjing, China using TIR and 3DPC data, Build. Environ. 116 (2017) 195–206.
[20] E. Shafiee, M. Faizi, S. Yazdanfar, M. Khanmohammadi, Assessment of the effect of living wall systems on the improvement of the urban heat island phenomenon, Build. Environ. 181 (2020), 106923.
[21] H. He, C.Y. Jim, Simulation of thermodynamic transmission in green roof ecosystem, Ecol. Model. 221 (24) (2010) 2949–2958.
[22] G. Pérez, L. Rincón, A. Vila, J.M. González, L.F. Cabeza, Green vertical systems for buildings as passive systems for energy savings, Appl. Energy 88 (12) (2011) 4854–4859.
[23] M. Fox, J. Morewood, T. Murphy, P. Lunt, S. Goodhew, Living wall systems for improved thermal performance of existing buildings, Build. Environ. 207 (2022) 108491.

[24] J. Coma, G. Pérez, A. de Gracia, S. Burés, M. Urrestarazu, L.F. Cabeza, Vertical greenery systems for energy savings in buildings: A comparative study between green walls and green facades, Build. Environ. 111 (2017) 228–237.
[25] A.k. Nayak, A. Hagishima, J. Tanimoto, A simplified numerical model for evaporative cooling by water spray over roof surfaces, Applied Thermal Engineering. 165 (2020) 114514.
[26] D.J. Sailor, A green roof model for building energy simulation programs, Energy Build. 40 (8) (2008) 1466–1478.
[27] J. Heusinger, D.J. Sailor, S. Weber, Modeling the reduction of urban excess heat by green roofs with respect to different irrigation scenarios, Build. Environ. 131 (2018) 174–183.
[28] I. Jaffal, S. Ouldboukhitine, R. Belarbi, A comprehensive study of the impact of green roofs on building energy performance, Renewable Energy 43 (2012) 157–164.
[29] S. Ouldboukhitine, R. Belarbi, I. Jaffal, A. Trabelsi, Assessment of green roof thermal behavior: A coupled heat and mass transfer model, Build. Environ. 46 (12) (2011) 2624–2631.
[30] E.P.D. Barrio, Analysis of the green roofs cooling potential in buildings, Energy Build. 27 (2) (1998) 179–193.
[31] J.W. Deardorff, Efficient prediction of ground surface temperature and moisture, with inclusion of a layer of vegetation, J. Geophys. Res. 83 (1978) 1889–1903.
[32] C. Feng, Q. Meng, Y. Zhang, Theoretical and experimental analysis of the energy balance of extensive green roofs, Energy Build. 42 (6) (2010) 959–965.
[33] R. Kumar, S.C. Kaushik, Performance evaluation of green roof and shading for thermal protection of buildings, Build. Environ. 40 (11) (2005) 1505–1511.
[34] T. Ayata, P.C. Tabares-Velasco, J. Srebric, An investigation of sensible heat fluxes at a green roof in a laboratory setup, Build. Environ. 46 (9) (2011) 1851–1861.
[35] D.J. Sailor, M. Hagos, An updated and expanded set of thermal property data for green roof growing media, Energy Build. 43 (9) (2011) 2298–2303.
[36] C.Y. Jim, S.W. Tsang, Modeling the heat diffusion process in the abiotic layers of green roofs, Energy Build. 43 (6) (2011) 1341–1350.
[37] Younes Chiba, Yacine Marif, Abdelali Boukaoud, Laid Meredef, Youcef Kaidi, Impact of green buildings on HVAC system located in Algeria, The Institute of Electrical and Electronics Engineers, Inc. (IEEE) Conference Proceedings. (Jan 1, 2018) 1.
[38] H. Zhao, F. Magoulès, A review on the prediction of building energy consumption, Renew. Sustain. Energy Rev. 16 (6) (2012) 3586–3592.
[39] E. Alexandri, P. Jones, Developing a one-dimensional heat and mass transfer algorithm for describing the effect of green roofs on the built environment: Comparison with experimental results, Build. Environ. 42 (8) (2007) 2835–2849.
[40] C.Y. Jim, S.W. Tsang, Biophysical properties and thermal performance of an intensive green roof, Build. Environ. 46 (6) (2011) 1263–1274.
[41] R.M. Lazzarin, F. Castellotti, F. Busato, Experimental measurements and numerical modelling of a green roof, Energy Build. 37 (12) (2005) 1260–1267.
[42] K. Chávez, D.P. Ruiz, M.J. Jiménez, Dynamic integrated method applied to assessing the in-situ thermal performance of walls and whole buildings, Robustness analysis supported by a benchmark set-up, Applied Thermal Engineering. 152 (2019) 287–307.
[43] G. Kotsiris, A. Androutsopoulos, E. Polychroni, P.A. Nektarios, Dynamic U-value estimation and energy simulation for green roofs, Energy Build. 45 (2012) 240–249.
[44] ASHRAE, Fundamentals volume of the *ASHRAE Handbook*. (2005).
[45] Royal Decree 314/2006 approving the Technical Building Code (Real Decreto 314/2006, de 17 de marzo, por el que se aprueba el Código Técnico de la Edificación), (2006).
[46] M.J. Moran, H.N. Shapiro, Fundamentals of engineering thermodynamics, Wiley, Hoboken, NJ, 2010.
[47] R. Stull, Wet-Bulb Temperature from Relative Humidity and Air Temperature, American Meteorological, Society. 50 (2011) 2267–2269.
[48] D. Prando, G. Gudmundsso, K. Gudmundson, K. Molinari, Global sensitivity analysis performance (2011).
[49] M. Rossi, V.M. Rocco, External walls design: The role of periodic thermal transmittance and internal areal heat capacity, Energy Build. 68 (2014) 732–740.
[50] Meteotest, METEONORM version 6.1. Meteeotest, (2008).
[51] AENOR, UNE-EN ISO 6946. Elementos y componentes de edificacion. Resistencia y transmitancia térmica. Método de cálculo, (1997).
[52] H.A.L. Van Dijk, G.P. Van der Linden, The PASSYS method for testing passive solar components, Build. Environ. 28 (2) (1993) 115–126.
[53] J.O. Lewis, Solar building—European Union Research and Development Programmes, Sol. Energy 58 (1-3) (1996) 127–135.
[54] P. Wouters, L. Vandaele, P. Voit, N. Fisch, The use of outdoor test cells for thermal and solar building research within the PASSYS project, Build. Environ. 28 (2) (1993) 107–113.
[55] M. Urrestarazu, S. Burés, Sustainble green walls in agriculture, J. Food Agric. Environ. 10 (1) (2012) 792–794.
[56] A. Erkoreka, J.J. Bloem, C. Escudero, K. Martin, J.M. Sala, Optimizing Full Scale Dynamic Testing of Building Components: Measurement Sensors and Monitoring Systems, Energy Procedia 78 (2015) 1738–1743.